17. FRAGMENTATION FUNCTIONS IN e^+e^- ANNIHILATION AND LEPTON-NUCLEON DIS

Revised August 2007 by O. Biebel (Ludwig-Maximilians-Universität, Munich, Germany), D. Milstead (Fysikum, Stockholms Universitet, Sweden), P. Nason (INFN, Sez. di Milano-Bicocca, Milan, Italy), and B.R. Webber (Cavendish Laboratory, Cambridge, UK). An extended version of the 2001 review can be found in Ref. 1.

17.1. Concept of fragmentation

17.1.1. *Introduction* :

Fragmentation functions are dimensionless functions that describe the final-state single-particle energy distributions in hard scattering processes, like e^+e^- annihilation or deep inelastic lepton-nucleon scattering, or high transverse momentum hadrons in photon-hadron and hadron-hadron collisions. The total e^+e^- fragmentation function for hadrons of type h in annihilation at c.m. energy $\sqrt{s}$, via an intermediate vector boson $V = \gamma/Z^0$, is defined as

$$F^h(x,s) = \frac{1}{\sigma_{\rm tot}}\frac{d\sigma}{dx}(e^+e^- \to V \to hX) \ , \tag{17.1}$$

where $x = 2E_h/\sqrt{s} \leq 1$ is the scaled hadron energy (in practice, the approximation $x = x_p = 2p_h/\sqrt{s}$ is often used). Its integral with respect to x gives the average multiplicity of those hadrons:

$$\langle n_h(s)\rangle = \int_0^1 dx\, F^h(x,s) \ , \tag{17.2}$$

Neglecting contributions suppressed by inverse powers of s, the fragmentation function (17.1) can be represented as a sum of contributions from the different parton types $i = u, \overline{u}, d, \overline{d}, \ldots, g$:

$$F^h(x,s) = \sum_i \int_x^1 \frac{dz}{z} C_i(s;z,\alpha_{\rm S}) D_i^h(x/z,s) \ . \tag{17.3}$$

where D_i^h are the parton fragmentation functions. At lowest order in $\alpha_{\rm S}$, the coefficient function C_g for gluons is zero, while for quarks $C_i = g_i(s)\delta(1-z)$, where $g_i(s)$ is the appropriate electroweak coupling. In particular, $g_i(s)$ is proportional to the charge-squared of parton i at $s \ll M_Z^2$, when weak effects can be neglected. In higher orders the coefficient functions and parton fragmentation functions are factorization-scheme dependent.

Parton fragmentation functions are analogous to the parton distributions in deep inelastic scattering (see sections on QCD and Structure Functions, 9 and 16 of this *Review*). In both cases, the simplest parton-model approach would predict a scale-independent x distribution. Furthermore, we obtain similar violations of this scaling behavior when QCD corrections are taken into account.

Fragmentation functions in lepton-hadron scattering and e^+e^- annihilation are complementary. Since e^+e^- annihilation results in a neutral off mass-shell photon or Z^0, fragmentation arising from a pure quark-antiquark system can be studied. Lepton-hadron scattering is a more complicated environment with which it is possible to study the influence on fragmentation functions from initial state QCD radiation, the partonic and spin structure of the hadron target, and the target remnant system.[1]

In lepton-hadron scattering, calling p the four momentum of the incoming hadron, and q the four momentum of the exchanged virtual boson, one can construct two independent kinematic invariants. One usually introduces $Q^2 = -q^2$ and defines $x_{\rm Bj} = Q^2/(2p \cdot q)$. Thus, there is a freedom in the choice of scale used to define a fragmentation function. For e^+e^-, the c.m. energy provides a natural choice of scale as twice the energy of each produced quark. For lepton-hadron interactions, fragmentation scales such as $Q = \sqrt{-q^2}$, or the invariant mass of the exchanged boson and target nucleon system $W = \sqrt{(p+q)^2} = \sqrt{m_h^2 + 2p \cdot q - Q^2}$ (where m_h is the incoming hadron mass), are typically used. Both W and Q can vary by several orders of magnitudes for a given c.m. energy, thus allowing the study of fragmentation in different environments by a single experiment, *e.g.*, in photoproduction the exchanged photon is quasi-real ($Q^2 \sim 0$) leading to processes akin to hadron-hadron scattering. In deep inelastic scattering (DIS)($Q^2 \gg 1$ GeV^2), using the Quark Parton Model (QPM), the hadronic fragments of the struck quark can be directly compared with quark fragmentation in e^+e^-. Results from lepton-hadron experiments quoted in this report primarily concern fragmentation in the DIS regime. Studies made by lepton-hadron experiments of fragmentation with photoproduction data containing high transverse momentum jets or particles are also reported, when these are directly comparable to DIS and e^+e^- results.

After the lepton-hadron interaction, the transverse momentum of the scattered lepton is balanced by the hadronic system. To remove the transverse momentum imbalance, many fragmentation studies have been performed in frames in which the target hadron and the exchanged boson are collinear. Two frames of reference are typically used which fulfill this condition.

The so-called hadronic c.m. frame (HCMS) is defined as the rest system of the exchanged boson and incoming hadron, with the z^*-axis defined along the direction of the exchanged boson. The $+z^*$ direction defines the so-called current region. Fragmentation measurements performed in the HCMS often use the Feynman-x variable $x_F = 2p_z^*/W$, where p_z^* is the longitudinal momentum of the particle in the HCMS. Since W is the invariant mass of the hadronic final state, x_F ranges between -1 and 1.

The Breit system [3] is connected to the HCMS by a longitudinal boost such that the time component of q becomes 0, so that $q = (0, 0, 0, -Q)$. In this frame, the target has three momentum $\vec{p} = (0, 0, Q/(2x_{\rm Bj}))$, as can be easily verified using the definition of $x_{\rm Bj}$. In the quark parton model, the struck parton has momentum $x_{\rm Bj} \cdot p$, and thus its longitudinal momentum is $Q/2$, which becomes $-Q/2$ after the collision.

[1] For a comprehensive review of the measurements and models of fragmentation in lepton-hadron scattering, see [2].

As compared with the HCMS, the current region of the Breit frame is more closely matched to the partonic scattering process, and is thus appropriate for direct comparisons of fragmentation functions in DIS with those from e^+e^- annihilation. The variable $x_p = 2p^*/Q$ is used at HERA for measurements of fragmentation functions in the Breit frame, ensuring directly comparable DIS and e^+e^- results.

17.2. Scaling violation

The evolution of the parton fragmentation function $D_i(x,t)$ with increasing scale $t = s$, like that of the parton distribution function $f_i(x,t)$ with $t = s$ (see Sec. 39 of this *Review*), is governed by the DGLAP equation [4]

$$t\frac{\partial}{\partial t}D_i(x,t) = \sum_j \int_x^1 \frac{dz}{z}\frac{\alpha_S}{2\pi}P_{ji}(z,\alpha_S)D_j(x/z,t)\ . \tag{17.4}$$

In analogy to DIS, in some cases an evolution equation for the fragmentation function F itself (Eq. (17.3)) can be derived from Eq. (17.4) [5]. Notice that the splitting function is now P_{ji} rather than P_{ij} since here D_j represents the fragmentation of the final parton. The splitting functions again have perturbative expansions of the form

$$P_{ji}(z,\alpha_S) = P_{ji}^{(0)}(z) + \frac{\alpha_S}{2\pi}P_{ji}^{(1)}(z) + \cdots \tag{17.5}$$

where the lowest-order functions $P_{ji}^{(0)}(z)$ are the same as those in deep inelastic scattering, but the higher-order terms [6,7] [2] are different. The effect of evolution is, however, the same in both cases: as the scale increases, one observes a scaling violation in which the x distribution is shifted towards lower values. This can be seen from Fig. 17.1.

The coefficient functions C_i in Eq. (17.3) and the splitting functions P_{ji} contain singularities at $z = 0$ and 1, which have important effects on fragmentation at small and large values of x, respectively. For details see *e.g.*, Ref. 1.

Quantitative results of studies of scaling violation in e^+e^- fragmentation are reported in [26–30]. The values of α_S obtained are consistent with the world average (see review on QCD in Sec. 9 of this *Review*).

Scaling violations in DIS are shown in Fig. 17.2 for both HCMS and Breit frame. In Fig. 17.2(a), the distribution in terms of $x_F = 2p_z/W$ shows for values of $x_F > 0.15$ a steeper slope in ep data than for the μp data, indicating the scaling violations. At smaller values of x_F in the current jet region, the multiplicity of particles substantially increases with W owing to the increased phase space available for the fragmentation process. The EMC data access both the current region and the region of the fragmenting target remnant system. At higher values of $|x_F|$, owing to the extended nature of the remnant, the multiplicity in the target region far exceeds that in the current region.

[2] There are misprints in the formulas in the published article [6]. The correct expressions can be found in the preprint version or in Ref. 8.

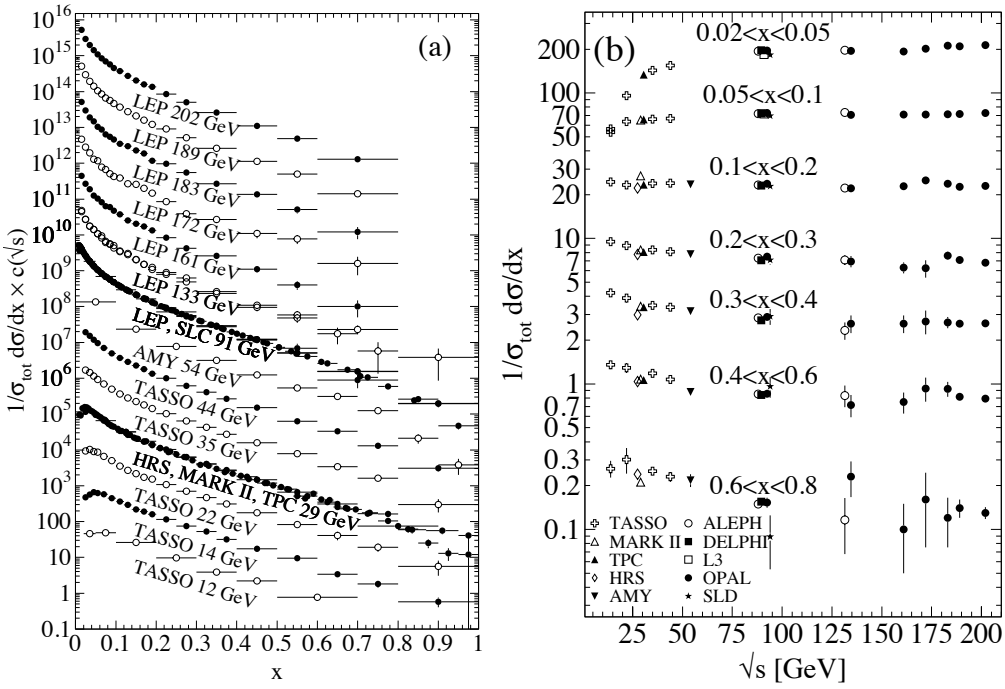

Figure 17.1: The e^+e^- fragmentation function for all charged particles is shown [9–25] (a) for different c.m. energies, $\sqrt{s}$, versus x and (b) for various ranges of x versus $\sqrt{s}$. For the purpose of plotting (a), the distributions were scaled by $c(\sqrt{s}) = 10^i$ where i is ranging from $i = 0$ ($\sqrt{s} = 12$ GeV) to $i = 13$ ($\sqrt{s} = 202$ GeV).

Owing to acceptance reasons, the remnant hemisphere of the HCMS is only accessible by the lower-energy fixed-target experiments.

Using hadrons from the current hemisphere in the Breit frame, measurements of fragmentation functions and the production properties of particles in ep scattering have been made by [35–40]. Fig. 17.2(b) compares results from ep scattering and e^+e^- experiments, the latter results are halved as they cover both event hemispheres. The agreement between the DIS and e^+e^- results is fairly good. However, processes in DIS which are not present in e^+e^- annihilation, such as boson-gluon fusion and initial state QCD radiation, can depopulate the current region. These effects become most prominent at low values of Q and x_p. When compared with e^+e^- annihilation data at $\sqrt{s} = 5.2$, 6.5 GeV [41], which are not shown here, the DIS particle rates tend to lie below those from e^+e^- annihilation. NLO QCD calculations [42], convoluted with fragmentation functions derived from e^+e^- data, have been tested against the HERA scaling violations data and provide a good description of the data in the kinematic regions in which the calculations are predictive [35,39,43].

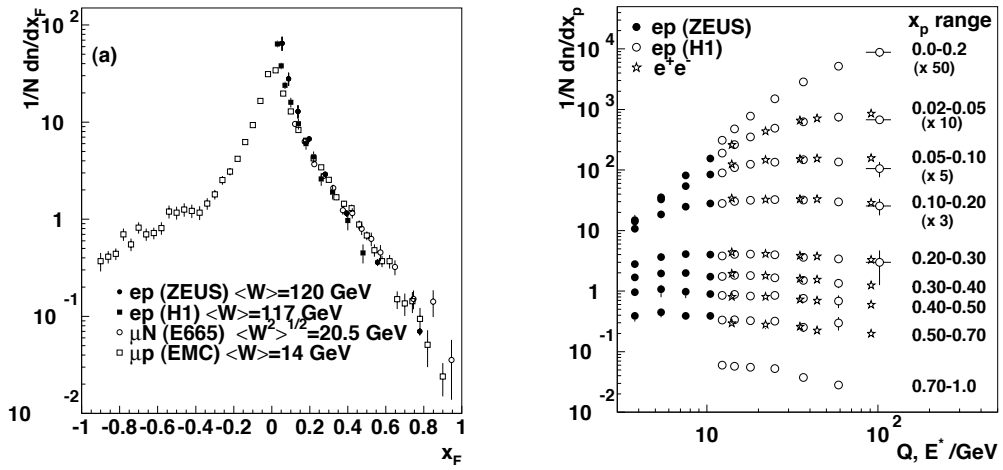

Figure 17.2: (a) The distribution $1/N \cdot dN/dx_F$ for all charged particles in DIS lepton-hadron experiments at different values of W, and measured in the HCMS [31–34]. (b) Scaling violations of the fragmentation function for all charged particles in the current region of the Breit frame of DIS [35,40] and in e^+e^- interactions [24,27]. The data are shown as a function of $\sqrt{s}$ for e^+e^- results, and as a function of Q for the DIS results, each within the same indicated intervals of the scaled momentum x_p. The data for the four lowest intervals of x_p are multiplied by factors 50, 10, 5, and 3, respectively for clarity.

17.3. Fragmentation functions for small particle momenta

As in the case of the parton distribution functions, the most common strategy for solving the evolution equations Eq. (17.4) is to take moments (Mellin transforms) with respect to x:

$$\tilde{D}(j,s) = \int_0^1 dx\; x^{j-1}\; D(x,s)\;. \tag{17.6}$$

The behavior of $\tilde{D}(j,s)$ away from $j=1$ determines the form of small-x fragmentation functions. Keeping the first three terms in a Taylor expansion around $j=1$ gives a simple Gaussian function of j which transforms by inverse Mellin transformation into a Gaussian in the variable $\xi \equiv \ln(1/x)$:

$$xD(x,s) \propto \exp\left[-\frac{1}{2\sigma^2}(\xi-\xi_p)^2\right]\;, \tag{17.7}$$

where the peak position is

$$\xi_p = \frac{1}{4b\alpha_S(s)} \simeq \frac{1}{4}\ln\left(\frac{s}{\Lambda^2}\right)\;, \tag{17.8}$$

with $b=(33-2n_f)/12\pi$ for n_f quark flavors and the width of the distribution of ξ is ($C_A=3$)

$$\sigma = \left(\frac{1}{24b}\sqrt{\frac{2\pi}{C_A\alpha_S^3(s)}}\right)^{\frac{1}{2}} \propto \left[\ln\left(\frac{s}{\Lambda^2}\right)\right]^{\frac{3}{4}}\;. \tag{17.9}$$

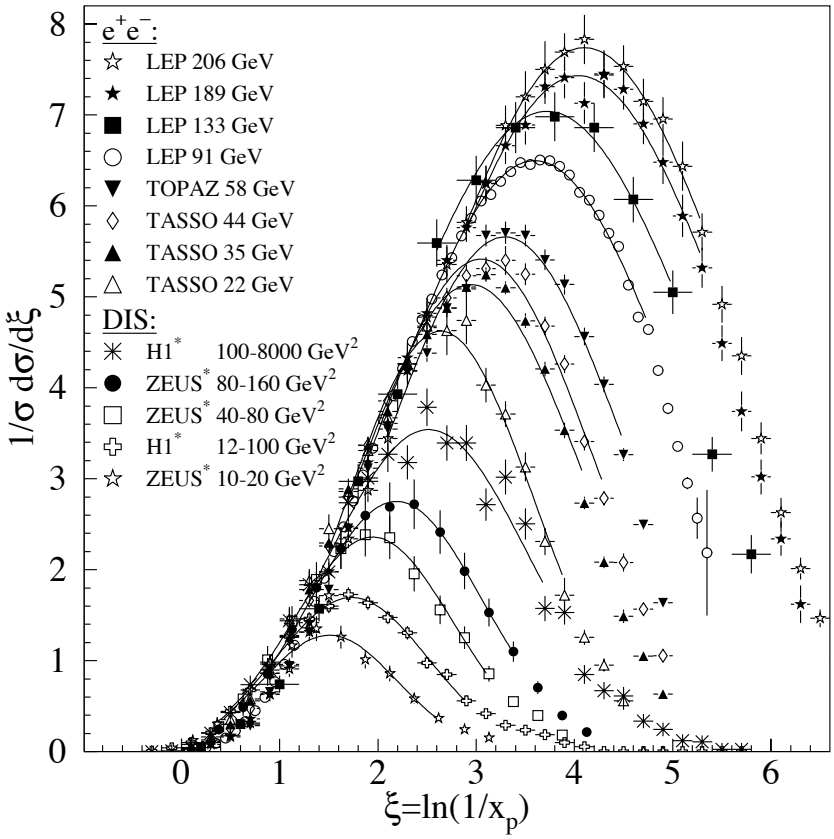

Figure 17.3: Distribution of $\xi = \ln(1/x_p)$ at several c.m. energies (e^+e^-) [9,10,14,17–20,24,46–49] and intervals of Q^2 (DIS) [38,39].[3] At each energy only one representative measurement is shown. For clarity some measurements at intermediate c.m. energies (e^+e^-) or Q^2 ranges (DIS) are not shown. The DIS measurements marked with * have been scaled by a factor of 2 for direct comparability with the e^+e^- results. Overlaid are fits of a simple Gaussian function for illustration.

Again, one can compute next-to-leading corrections to these predictions. In the method of [44], the corrections are included in an analytical form known as the 'modified leading logarithmic approximation' (MLLA). Alternatively they can be used to compute the higher moment corrections to the Gaussian form Eq. (17.7) [45]. Fig. 17.3 shows the ξ distribution for charged particles produced in the current region of the Breit frame in DIS interactions,[3] and in e^+e^- annihilation. As expected from Eq. (17.7), Eq. (17.8), and Eq. (17.9), the distributions have a Gaussian shape, with the peak position and area becoming progressively larger with c.m. energy (e^+e^-) and Q^2 (DIS).

[3] Dominant systematic errors used for the results of [39] are according to this reference 10% for $x_p < 0.3$ and increase up to 30% for large x_p.

The predicted energy dependence Eq. (17.8) of the peak in the ξ distribution is a striking illustration of soft gluon coherence, which is the origin of the suppression of hadron production at small x. Of course, a decrease at very small x is expected on purely kinematical grounds, but this would occur at particle energies proportional to their masses, *i.e.*, at $x \propto m/\sqrt{s}$ and hence $\xi \sim \frac{1}{2}\ln s$. Thus, if the suppression were purely kinematic, the peak position ξ_p would vary twice as rapidly with energy, which is ruled out by the data (see Fig. 17.4). The e^+e^- and DIS data agree well with each other, demonstrating the universality of hadronization. The MLLA prediction describes the data. Measurements of the higher moments of the ξ distribution in e^+e^- [24,49–51] and DIS [39] have also been made and show consistency with each other.

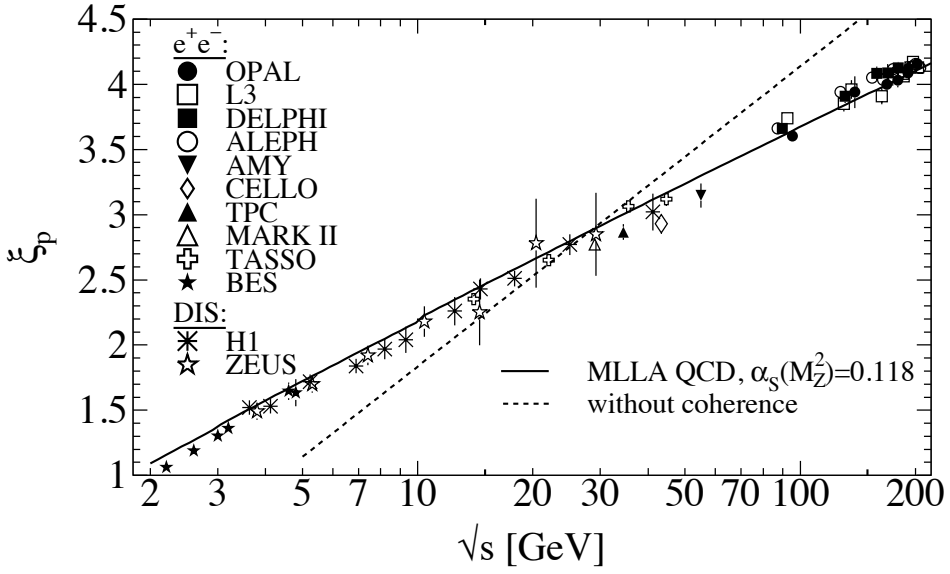

Figure 17.4: Evolution of the peak position, ξ_p, of the ξ distribution with the c.m. energy $\sqrt{s}$. The MLLA QCD prediction (solid) using $\alpha_S(s = M_Z^2) = 0.118$ and the expectation without gluon coherence (dashed) are superimposed to the data [9,11,14,16–18,20,24,37,38,47,48,50,52–59].

17.3.1. *Longitudinal Fragmentation* :

In the process $e^+e^- \to V \to hX$, the joint distribution in the energy fraction x and the angle θ between the observed hadron h and the incoming electron beam has the general form

$$\frac{1}{\sigma_{\rm tot}}\frac{d^2\sigma}{dx\, d\cos\theta} = \frac{3}{8}(1+\cos^2\theta)\, F_T(x) + \frac{3}{4}\sin^2\theta\, F_L(x) + \frac{3}{4}\cos\theta\, F_A(x)\ , \qquad (17.10)$$

where F_T, F_L and F_A are respectively the transverse, longitudinal and asymmetric fragmentation functions. All these functions also depend on the c.m. energy $\sqrt{s}$.

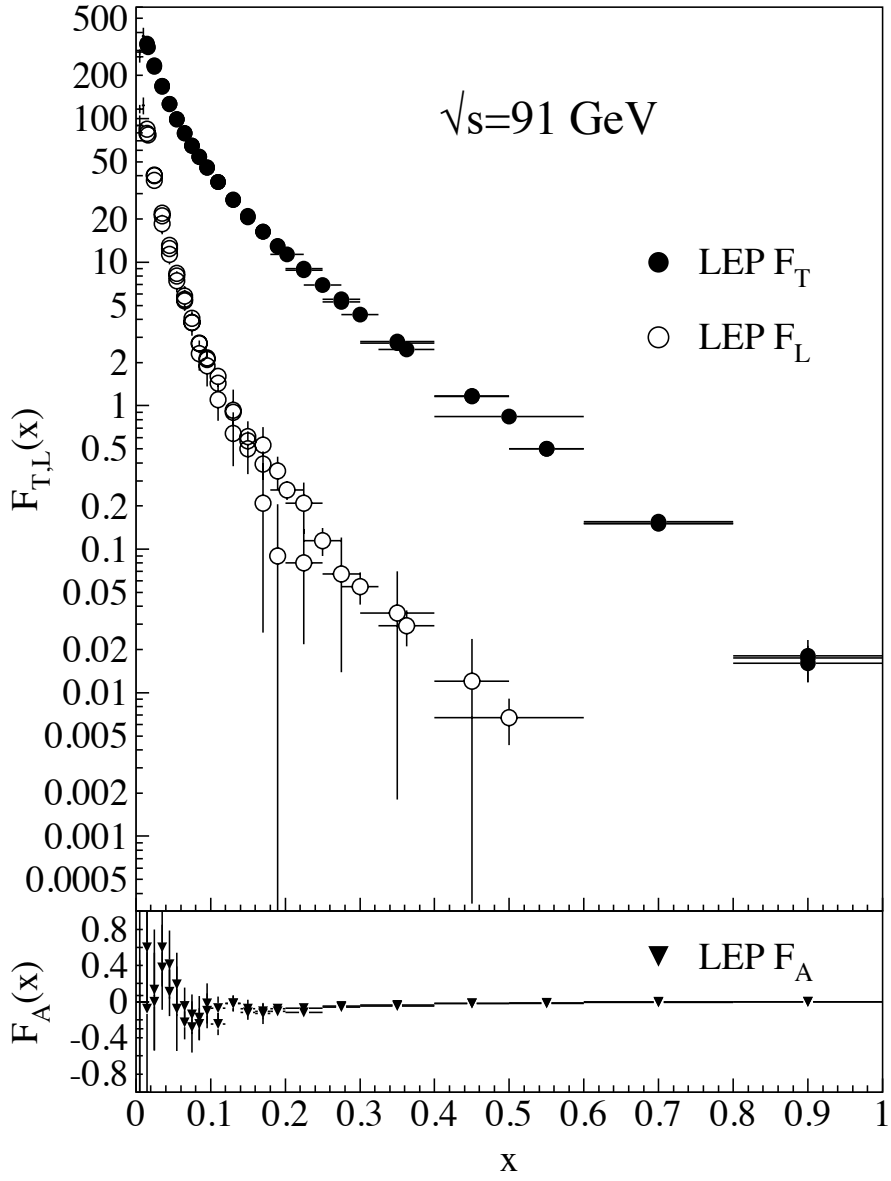

Figure 17.5: Transverse (F_T), longitudinal (F_L), and asymmetric (F_A) fragmentation functions are shown [12,26,60]. Data points with relative errors greater than 100% are omitted.

Eq. (17.10) is the most general form of the inclusive single particle production from the decay of a massive vector boson [5]. As their names imply, F_T and F_L represent the contributions from virtual bosons polarized transversely or longitudinally with respect to the direction of motion of the hadron h. F_A is a parity-violating contribution which comes from the interference between vector and axial vector contributions. Integrating over all angles, we obtain the total fragmentation function, $F = F_T + F_L$. Each of these

functions can be represented as a convolution of the parton fragmentation functions D_i with appropriate coefficient functions $C_i^{\mathrm{T,L,A}}$ as in Eq. (17.3). This representation works in the high energy limit. As $x \cdot \sqrt{s}/2$ approaches hadronic scales $\simeq m_\rho$, power suppressed effects can no longer be neglected, and the fragmentation function formalism no longer accounts correctly for the separation of F_T, F_L, and F_A. In Fig. 17.5, F_T, F_L, and F_A measured at $\sqrt{s} = 91$ GeV are shown.

17.4. Gluon fragmentation

The gluon fragmentation function $D_g(x)$ can be extracted from the longitudinal fragmentation function defined in Eq. (17.10). Since the coefficient functions C_i^{L} for quarks and gluons are comparable in $\mathcal{O}(\alpha_{\mathrm{S}})$, F_L can be expressed in terms of F_T and D_g which allows one to obtain D_g from the measured F_L and F_T, see *e.g.*, [1] for details. At NLO, *i.e.*, $\mathcal{O}(\alpha_S^2)$ coefficient functions C_i, quark fragmentation is dominant in F_L over a large part of the kinematic range, see *e.g.*, [61]. This leaves some sensitivity of F_L to D_g, but further constraints will be needed, for instance from hadro-production in deep-inelastic scattering.

D_g can also be deduced from the fragmentation of three-jet events in which the gluon jet is identified, for example, by tagging the other two jets with heavy quark decays. To leading order, the measured distributions of $x = E_{\mathrm{had}}/E_{\mathrm{jet}}$ for particles in gluon jets can be identified directly with the gluon fragmentation functions $D_g(x)$. The experimentally measured gluon fragmentation functions are shown in Fig. 17.6.

17.5. Spin-dependent fragmentation

Measurements of hadron production in polarized lepton-hadron scattering are used principally in the determination of polarized parton densities from DIS interactions with longitudinally polarized targets [63–65]. Since flavor-dependent fragmentation functions derived from the $e^+e^- \to hX$ can give significantly different flavor contributions [66–71], experiments use string fragmentation in JETSET [72], which is tuned to describe their own identified particle data, and those measured by other low energy DIS experiments.

Polarized scattering presents the possibility to measure the spin transfer from the struck quark to the final hadron, and thus develop spin-dependent fragmentation functions [73,74]. These are useful in the study of the quark transversity distribution [75], which describes the probability of finding a transversely polarized quark with its spin aligned or anti-aligned with the spin of a transversely polarized nucleon. The transversity function is chiral-odd, and therefore not accessible through measurements of inclusive lepton-hadron scattering. Semi-inclusive DIS, in which another chiral-odd observable may be involved, provides a valuable tool to probe transversity. The Collins fragmentation function [76] relates the transverse polarization of the quark to that of the final hadron. It is chiral-odd and naive T-odd, leading to a characteristic single spin asymmetry in the azimuthal angular distribution of the produced hadron in the hadron scattering plane. A number of experiments have measured this asymmetry (see *e.g.*, [77]). However, these studies were unable to distinguish between processes due to transversity in conjunction with the Collins fragmentation with other processes requiring non-polarized fragmentation

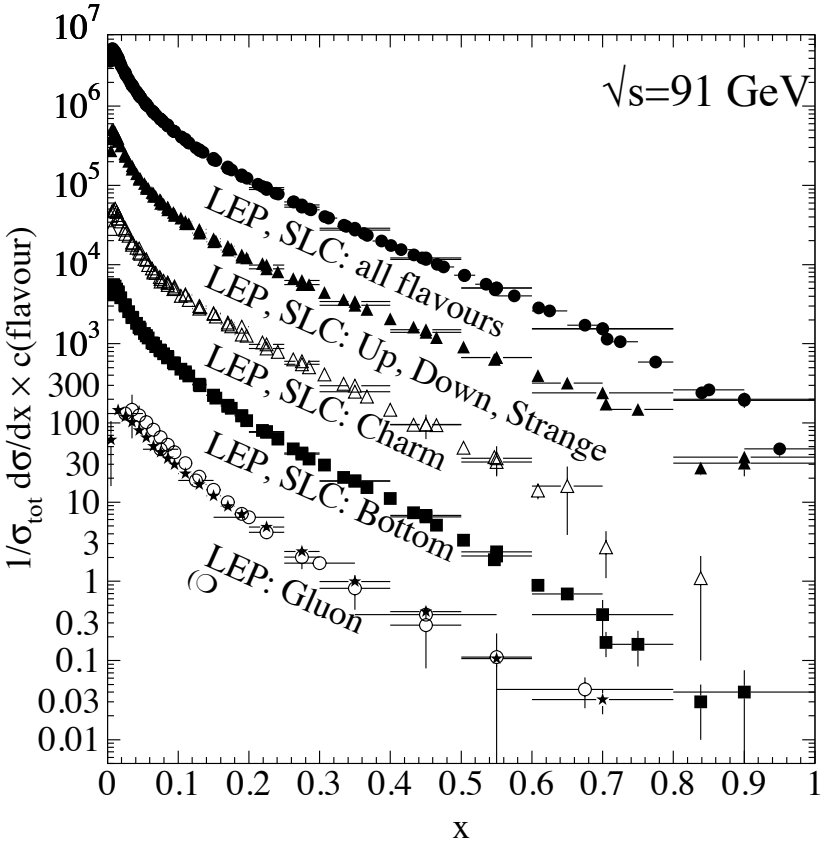

Figure 17.6: Comparison of the charged-particle and the flavor-dependent e^+e^- fragmentation functions obtained at $\sqrt{s} = 91$ GeV. The data [10,12,14,15,19,21] and [22,28,60,62] are shown for the inclusive, light (up, down, strange) quarks, charm quark, bottom quark, and the gluon versus x. For the purpose of plotting, the distributions were scaled by $c(\text{flavor}) = 10^i$, where i is ranging from $i = 0$ (Gluon) to $i = 4$ (all flavors).

functions, such as the Sivers mechanism [78]. However, the HERMES and COMPASS collaborations have made early studies of the Collins and Sivers asymmetries using a transversely polarized target [79–81].

17.6. Fragmentation models

Although the scaling violation can be calculated perturbatively, the actual form of the parton fragmentation functions is non-perturbative. Perturbative evolution gives rise to a shower of quarks and gluons (partons). Phenomenological schemes are then used to model the carry-over of parton momenta and flavor to the hadrons. Two of the very popular models are the *string fragmentation* [82,83], implemented in the JETSET [72] and UCLA [84] Monte Carlo event generation programs, and the *cluster fragmentation* of the HERWIG Monte Carlo event generator [85].

17.6.1. ***String fragmentation*** : The string-fragmentation scheme considers the color field between the partons, *i.e.*, quarks and gluons, to be the fragmenting entity rather than the partons themselves. The string can be viewed as a color flux tube formed by gluon self-interaction as two colored partons move apart. Energetic gluon emission is regarded as energy-momentum carrying "kinks" on the string. When the energy stored in the string is sufficient, a $q\overline{q}$ pair may be created from the vacuum. Thus, the string breaks up repeatedly into color singlet systems, as long as the invariant mass of the string pieces exceeds the on-shell mass of a hadron. The $q\overline{q}$ pairs are created according to the probability of a tunneling process $\exp(-\pi m^2_{q,\perp}/\kappa)$, which depends on the transverse mass squared $m^2_{q,\perp} \equiv m^2_q + p^2_{q,\perp}$ and the string tension $\kappa \approx 1$ GeV/fm. The transverse momentum $p_{q,\perp}$ is locally compensated between quark and antiquark. Due to the dependence on the parton mass, m_q, and/or hadron mass, m_h, the production of strange and, in particular, heavy-quark hadrons is suppressed. The light-cone momentum fraction $z = (E + p_\parallel)_h/(E + p)_q$, where $p_\parallel$ is the momentum of the formed hadron h along the direction of the quark q, is given by the string-fragmentation function

$$f(z) \sim \frac{1}{z}(1-z)^a \exp\left(-\frac{bm^2_{h,\perp}}{z}\right) , \tag{17.11}$$

where a and b are free parameters. These parameters need to be adjusted to bring the fragmentation into accordance with measured data, *e.g.*, $a = 0.11$ and $b = 0.52$ GeV^{-2} as determined in Ref. 86 (for an overview on tuned parameters see Ref. 87).

17.6.2. ***Cluster fragmentation*** : Assuming a local compensation of color based on the *pre-confinement* property of perturbative QCD [88], the remaining gluons at the end of the parton shower evolution are split non-perturbatively into quark-antiquark pairs. Color singlet clusters of typical mass of a couple of GeV are then formed from quark and antiquark of color-connected splittings. These clusters decay directly into two hadrons unless they are either too heavy (relative to an adjustable parameter `CLMAX`, default value 3.35 GeV), when they decay into two clusters, or too light, in which case a cluster decays into a single hadron, requiring a small rearrangement of energy and momentum with neighboring clusters. The decay of a cluster into two hadrons is assumed to be isotropic in the rest frame of the cluster except if a perturbative-formed quark is involved. A decay channel is chosen based on the phase-space probability, the density of states, and the spin degeneracy of the hadrons. Cluster fragmentation has a compact description with few parameters, due to the phase-space dominance in the hadron formation.

17.7. Fragmentation into identified particles

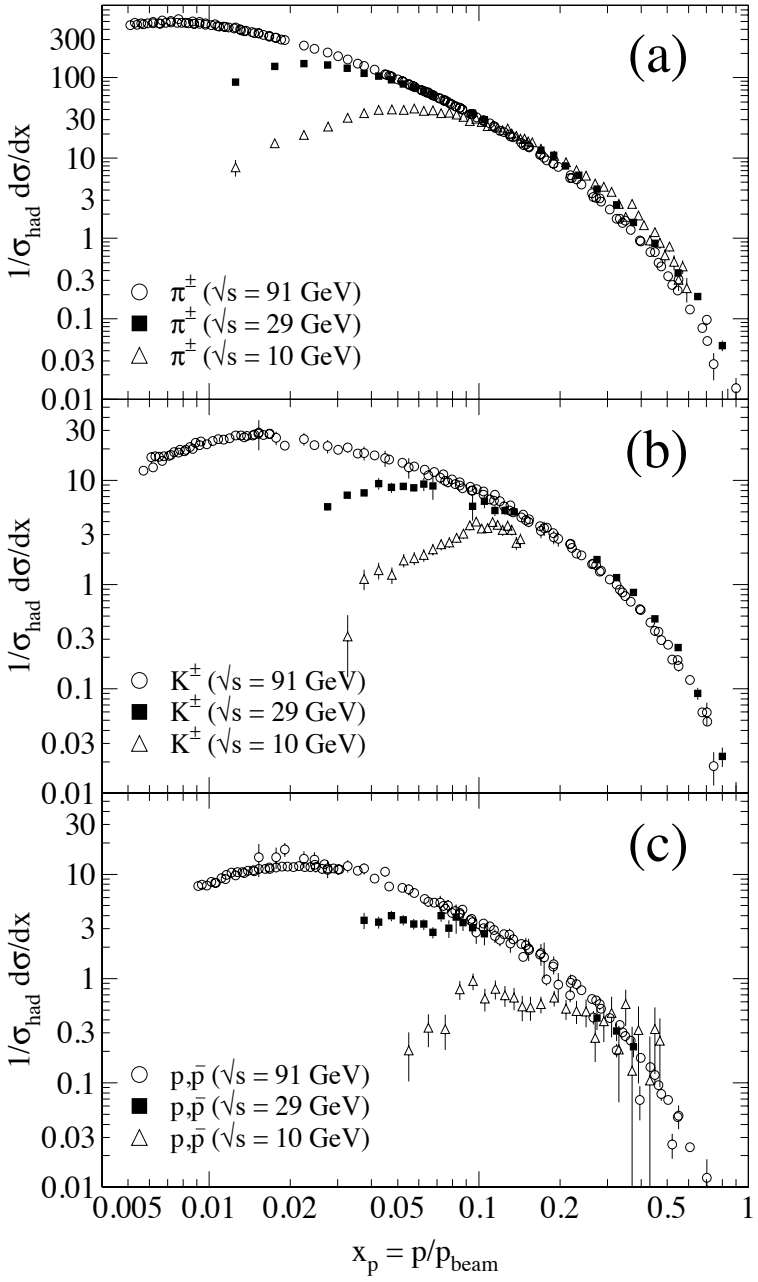

Figure 17.7: Scaled momentum spectra of (a) $\pi^\pm$, (b) $K^\pm$, and (c) $p/\overline{p}$ at $\sqrt{s} = 10$, 29, and 91 GeV are shown [22,25,56,89].

A great wealth of measurements of e^+e^- fragmentation into identified particles exists. A collection of references to find data on the fragmentation into identified particles is

given for Table 40.1. As representatives of all the data, Fig. 17.7 shows fragmentation functions as the scaled momentum spectra of charged particles at several c.m. energies. Heavy flavor particles are dealt with separately in Sect. 17.8.

The measured fragmentation functions are solutions to the DGLAP equation (17.4), but need to be parametrized at some initial scale t_0 (usually 2 GeV^2 for light quarks and gluons). A general parametrization is [90]

$$D_{p\to h}(x,t_0) = Nx^{\alpha}(1-x)^{\beta}\left(1+\frac{\gamma}{x}\right) \ , \tag{17.12}$$

where the normalization N, and the parameters α, β, and γ in general depend on the energy scale t_0, and also on the type of the parton, p, and the hadron, h. Frequently the term involving γ is left out [66–70]. The parameters of Eq. (17.12), listed in [66–70], were obtained by fitting data on various hadron types for different combinations of partons and hadrons in $p \to h$ in the range $\sqrt{s} \approx 5$ - 200 GeV.

Many studies have been made of identified particles produced in lepton-hadron scattering, although fewer particle species have been measured than in e^+e^- collisions. References [91–96] and [97–101] are representative of the data from fixed target and ep collider experiments.

Fig. 17.8(a) compares lower-energy fixed-target and HERA data on strangeness production, showing that the HERA spectra have substantially increased multiplicities, albeit with insufficient statistical precision to study scaling violations. The fixed-target data show that the Λ rate substantially exceeds the $\overline{\Lambda}$ rate in the remnant region, owing to the conserved baryon number from the baryon target. Fig. 17.8(b) shows neutral and charged pion fragmentation functions $1/N \cdot dn/dz$, where z is defined as the ratio of the pion energy to that of the exchanged boson, both measured in the laboratory frame. Results are shown from HERMES and the EMC experiments, where HERMES data have been evolved with NLO QCD to $\langle Q^2 \rangle = 25$ GeV^2 in order to be consistent with the EMC. Each of the experiments uses various kinematic cuts to ensure that the measured particles lie in the region which is expected to be associated with the struck quark. In the DIS kinematic regime accessed at these experiments, and over the range in z shown in Fig. 17.8, the z and x_F variables have similar values [31]. The precision data on identified particles can be used in the study of the quark flavor content of the proton [102].

Data on identified particle production are also useful in studying the universality of jet fragmentation in e^+e^- and DIS. The strangeness suppression factor γ_s, as derived principally from tuning the Lund string model [83] within JETSET [72], is typically found to be around 0.3 in e^+e^- experiments [46], although values closer to 0.2 [103] have also been obtained. The converse is true for DIS experiments, with the tendency from HERA [97,99] and recent fixed-target measurements [91] of light strange particle production, to support a stronger suppression ($\gamma_s \approx 0.2$), although values close to 0.3 have also been obtained [104,105].

However, when comparing the description of QCD-based models for lepton-hadron interactions and e^+e^- collisions, it is important to note that the overall description by event generators of inclusively produced hadronic final states is more precise in

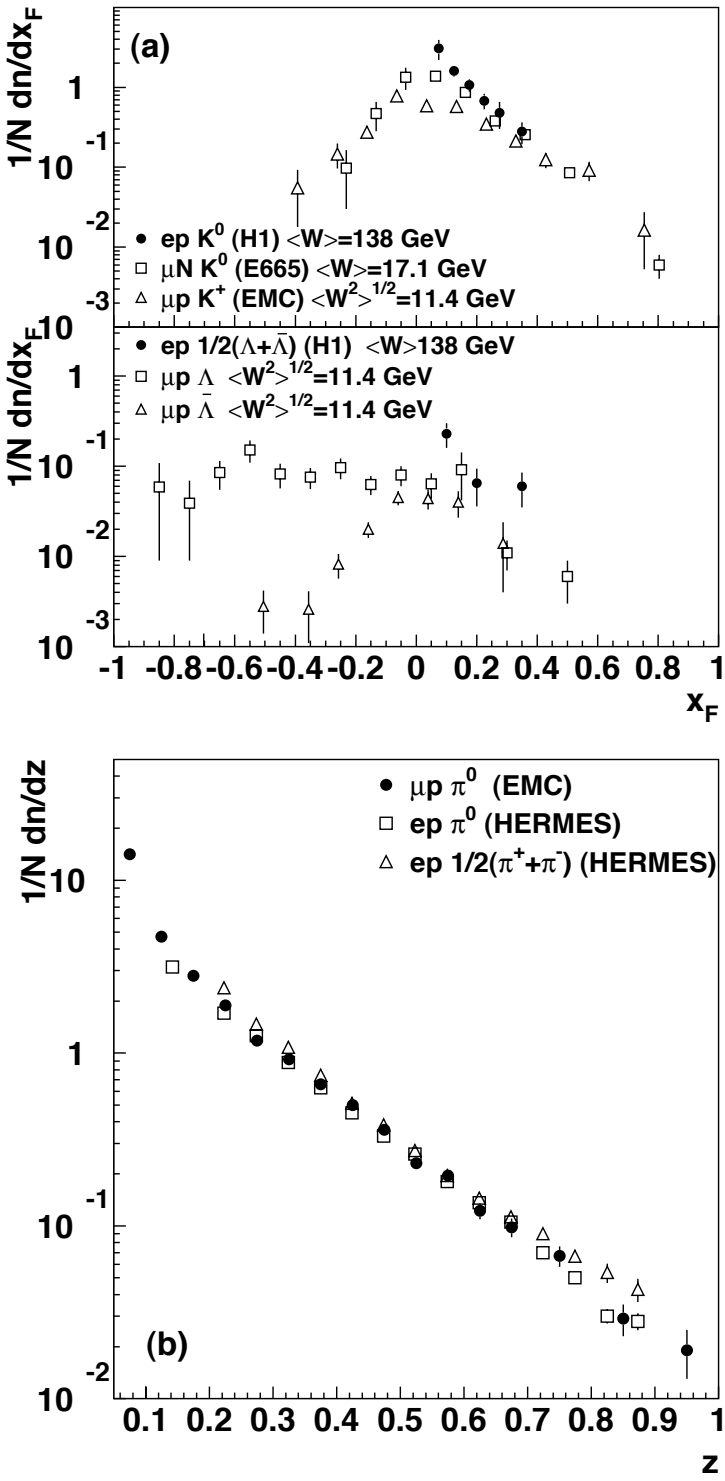

Figure 17.8: (a) $1/N \cdot \mathrm{d}n/\mathrm{d}x_F$ for identified strange particles in DIS at various values of W [91,94,97]. (b) $1/N \cdot \mathrm{d}n/\mathrm{d}z$ for measurements of pions from fixed-target DIS experiment [92,95,96].

e^+e^- collisions than lepton-hadron interactions [106]. Predictions of particle rates in lepton-hadron scattering are affected by uncertainties in the modeling of the parton composition of the proton and photon, the extended target remnant, and initial and final state QCD radiation. Furthermore, the tuning of event generators for e^+e^- collisions is typically based on a larger set of parameters and uses more observables [46] than are used when optimizing models for lepton-hadron data [107].

17.8. Heavy quark fragmentation

It was recognized very early [108] that a heavy flavored meson should retain a large fraction of the momentum of the primordial heavy quark, and therefore its fragmentation function should be much harder than that of a light hadron. In the limit of a very heavy quark, one expects the fragmentation function for a heavy quark to go into any heavy hadron to be peaked near 1.

When the heavy quark is produced at a momentum much larger than its mass, one expects important perturbative effects, enhanced by powers of the logarithm of the transverse momentum over the heavy quark mass, to intervene and modify the shape of the fragmentation function. In leading logarithmic order (*i.e.*, including all powers of $\alpha_S \log m_Q/p_T$), the total (*i.e.*, summed over all hadron types) perturbative fragmentation function is simply obtained by solving the leading evolution equation for fragmentation functions, Eq. (17.4), with the initial condition at a scale $\mu^2 = m_Q^2$ given by $D_Q(z, m_Q^2) = \delta(1-z)$ and $D_i(z, m_Q^2) = 0$ for $i \neq Q$ (the notation $D_i(z)$, stands for the probability to produce a heavy quark Q from parton i with a fraction z of the parton momentum).

Several extensions of the leading logarithmic result have appeared in the literature. Next-to-leading-log (NLL) order results for the perturbative heavy quark fragmentation function have been obtained in Ref. 109. At large z, phase space for gluon radiation is suppressed. This exposes large perturbative corrections due to the incomplete cancellation of real gluon radiation and virtual gluon exchange (Sudakov effects), which should be resumed in order to get accurate results. A leading-log (LL) resummation formula has been obtained in [109,110]. Next-to-leading-log resummation has been performed in Ref. 111. Fixed-order calculations of the fragmentation function at order α_S^2 in e^+e^- annihilation have appeared in Ref. 112. This result does not include terms of order $(\alpha_S \log s/m^2)^k$ and $\alpha_S(\alpha_S \log s/m^2)^k$, but it does include correctly all terms up to the order α_S^2, including terms without any logarithmic enhancements. The result of Ref. 109 for the perturbative initial condition of the heavy quark fragmentation function has been extended to NNLO (next-to-next-to-leading order) in Ref. 113. Other ingredients (*i.e.*, NNLO single inclusive production cross sections for light quarks, and NNLO evolution for fragmentation function) are, however, still missing for a full NNLO analysis of heavy-flavor fragmentation functions.

Inclusion of non-perturbative effects in the calculation of the heavy-quark fragmentation function is done in practice by convolving the perturbative result with a phenomenological

non-perturbative form. Among the most popular parameterizations we have the following:

$$\text{Peterson } \textit{et al.} \text{ [114]}: \quad D_{\rm np}(z) \propto \frac{1}{z}\left(1-\frac{1}{z}-\frac{\epsilon}{1-z}\right)^{-2}, \tag{17.13}$$

$$\text{Kartvelishvili } \textit{et al.} \text{ [115]}: \quad D_{\rm np}(z) \propto z^{\alpha}(1-z), \tag{17.14}$$

$$\text{Collins\&Spiller [116]}: \quad D_{\rm np}(z) \propto \left(\frac{1-z}{z}+\frac{(2-z)\epsilon_C}{1-z}\right)\times (1+z^2)\left(1-\frac{1}{z}-\frac{\epsilon_C}{1-z}\right)^{-2} \tag{17.15}$$

$$\text{Colangelo\&Nason [117]}: \quad D_{\rm np}(z) \propto (1-z)^{\alpha} z^{\beta} \tag{17.16}$$

$$\text{Bowler [118]}: \quad D_{\rm np}(z) \propto z^{-(1+bm_{h,\perp}^2)}(1-z)^{a}\exp\left(-\frac{bm_{h,\perp}^2}{z}\right) \tag{17.17}$$

$$\text{Braaten } \textit{et al.} \text{ [119]}: \quad \text{(see Eq. (31), (32) in [119])}, \tag{17.18}$$

where ϵ, ϵ_C, a, $bm_{h,\perp}^2$, α, and β are non-perturbative parameters, depending upon the heavy hadron considered. In general, the non-perturbative parameters entering the non-perturbative forms do not have an absolute meaning. They are fitted together with some model of hard radiation, which can be either a shower Monte Carlo, a leading-log or NLL calculation (which may or may not include Sudakov resummation), or a fixed order calculation. In [112], for example, the Peterson *et al.* [114] ϵ parameter for charm and bottom production is fitted from the measured distributions of refs. [120,121] for charm, and of [122] for bottom. If the leading-logarithmic approximation (LLA) is used for the perturbative part, one finds $\epsilon_c \approx 0.05$ and $\epsilon_b \approx 0.006$; if a second order calculation is used one finds $\epsilon_c \approx 0.035$ and $\epsilon_b \approx 0.0033$; if a NLLO calculation is used instead, one finds $\epsilon_c \approx 0.022$ and $\epsilon_b \approx 0.0023$. The larger values found in the LL approximation are consistent with what is obtained in the context of parton shower models [123], as expected. The ϵ parameter for charm and bottom scales roughly with the inverse square of the heavy flavor mass. This behavior can be justified by several arguments [108,124,125]. It can be used to relate the non-perturbative parts of the fragmentation functions of charm and bottom quarks [112,117,126].

17.8.1. ***Charm quark fragmentation*** : High statistics data for charmed mesons production near the Υ resonance (excluding decay products of B mesons) have been published [127,128]. They include results for D and D^*, D_s (see also [129,130]) and Λ_c. Shown in Fig. 17.9(a) are the CLEO and BELLE inclusive cross-sections times branching ratio $\mathcal{B}$, $s \cdot \mathcal{B}d\sigma/dx_p$, for the production of D^0 and D^{*+}. The variable x_p approximates the light-cone momentum fraction z in Eq. (17.13), but is not identical to it. The two measurements are fairly consistent with each other.

The branching ratio $\mathcal{B}$ represents $D^0 \to K^-\pi^+$ for the D^0 results and for the D^{*+} the product branching fraction: $D^{*+} \to D^0\pi^+$, $D^0 \to K^-\pi^+$. Older studies are reported in Refs. [121,132]. Charmed meson spectra on the Z peak have been

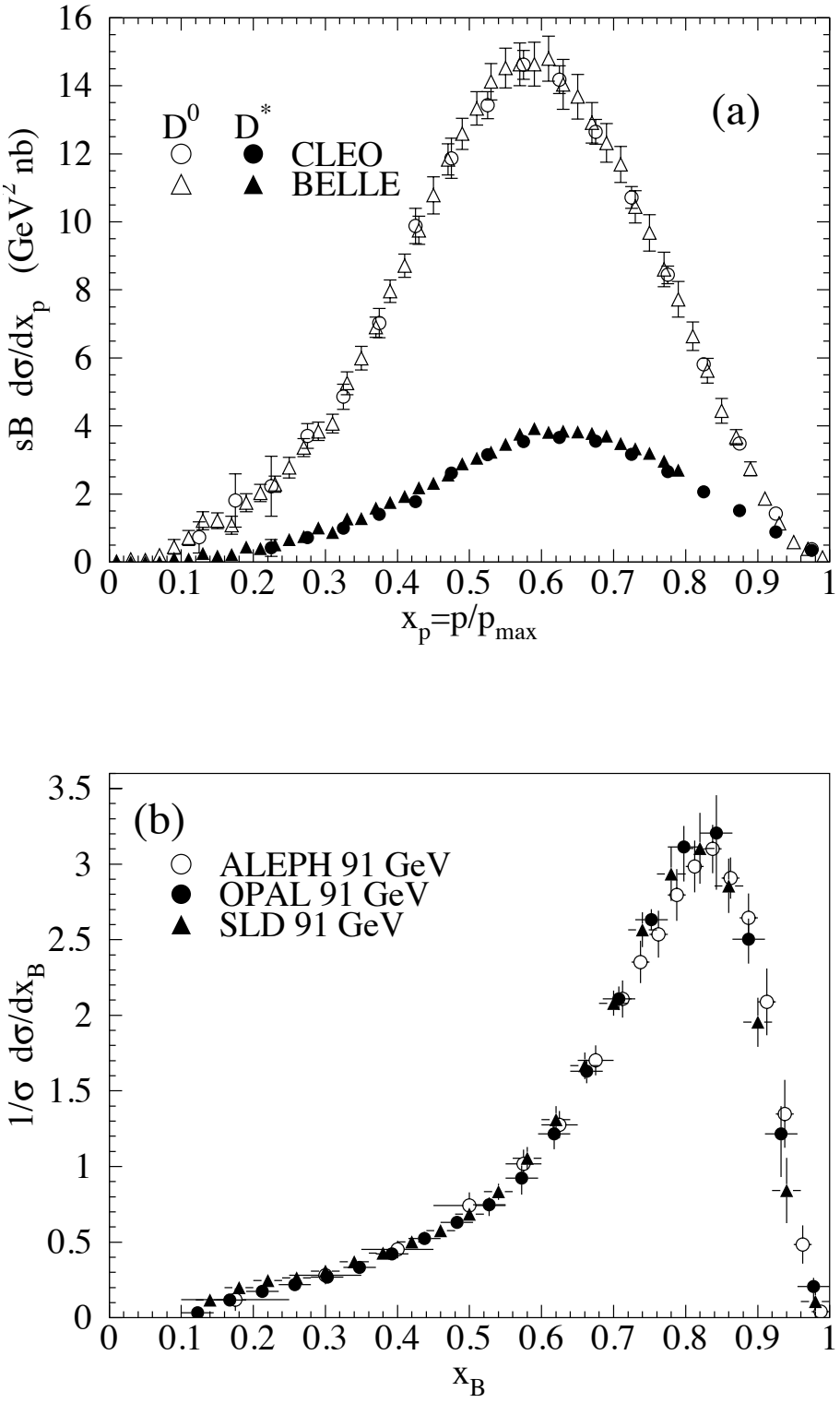

Figure 17.9: (a) Efficiency-corrected inclusive cross-section measurements for the production of D^0 and D^{*+} in e^+e^- measurements at $\sqrt{s} \approx 10.6$ GeV, excluding B decay products [127,128]. (b) Measured e^+e^- fragmentation function of b quarks into B hadrons at $\sqrt{s} \approx 91$ GeV [131].

published by OPAL and ALEPH [86,133]. The relative production fractions of the various hadron species should be process-independent at high energies according to QCD factorization. Combining results near the $\Upsilon(4S)$ from Refs. [127,128,130,132,134], neglecting the gluon splitting contribution, which is negligible at these energies, we obtain $f(c \to D^0) = 0.565 \pm 0.032$, $f(c \to D^+) = 0.246 \pm 0.020$, $f(c \to D_s^+) = 0.080 \pm 0.017$, $f(c \to \Lambda_c^+) = 0.094 \pm 0.035$, $f(c \to D^{*0}) = 0.213 \pm 0.024$, $f(c \to D^{*+}) = 0.224 \pm 0.028$, and $f(c \to D_s^{*+}) = 0.061 \pm 0.018$, in good agreement with those reported by LEP and SLD (see App. B of Ref. 135). Here, f is the fraction of produced charm quarks that hadronize into the respective hadron, eventually including decays of short-lived resonances.

As is well known, the large (isospin violating) difference in D^+ and D^0 production is well understood as a consequence of the fact that D^* mesons have a mass that is accidentally very near the sum of the D and the pion mass. The small isospin violating mass differences between states of different charge are such that both the D^{*+} and the D^{*0} can decay into the D^0 with large branching fractions, while only the D^{*+} can decay to a D^+, with a relatively small branching. If we can assume that similar accidents do not happen with higher resonances, we can conclude that D^{*+} and D^{*-} are produced with the same rate, and that D^0 and D^+ not coming from D^* decays are also produced with the same rate. The data are at present consistent with this view within errors, although it would seem to favor a $f(c \to D^{*+})$ larger than $f(c \to D^{*0})$. BELLE [128] publishes a ratio $(D^{*+} + D^{*0})/(D^+ + D^0) = 0.527 \pm 0.013 \pm 0.024$, so that the ratio of primary to total D is $0.473 \pm 0.013 \pm 0.024$.

Given the high precision of CLEO's and BELLE's data, it is difficult to obtain good fits of the inclusive cross-sections with the simple parameterizations generally used [114–118], see Ref. 128. It is, however, still possible to obtain good fits to the data using relatively simple forms. In the context of a QCD calculation of the fragmentation function, including NLO initial condition, evolution and coefficient functions, and NLL resummation of Sudakov effects in the initial condition and in the coefficient functions, it was shown in Ref. 136 that a superposition of the form proposed in Ref. 117 and a delta function for the description of D^*'s and primary D mesons yields very good fits to CLEO and BELLE data. In the same work it is shown, however, that one cannot fit simultaneously CLEO/BELLE and ALEPH data in a pure perturbative QCD framework. This fact could be interpreted in terms of power corrections to the coefficient functions, with a suppression $1/Q^2$ (compatible with the result of Ref. 137) or $1/Q$ (similar to the form proposed in Ref. 5).

Charm quark production has also been extensively studied at HERA by the H1 and ZEUS collaborations. Measurements have been made of $D^{*\pm}$, $D^{\pm}$, and $D_s^{\pm}$ mesons [138–142] and the Λ_c baryon [141]. Various fragmentation quantities have been extracted, some of which are shown in Table 17.1 as measured by H1 and ZEUS, along with averages of these quantities as obtained from e^+e^- data.

Table 17.1: Measurements of fragmentation ratios from *ep* [140,142] and e^+e^- experiments [143]. $R_{u/d}$ is ratio of neutral to charged D-mesons, γ_s is the strangeness suppression factor in charm fragmentation, and P_v^d is the fraction of charged D-mesons produced in a vector state.

	$R_{u/d}$
H1	1.26 ± 0.20 (stat.)± 0.11 (syst.)± 0.04 (br. $\oplus$ theo.)
ZEUS	1.22 ± 0.11 (stat.)$^{+0.05}_{-0.02}$ (syst.) ± 0.03 (br.)
e^+e^- av.	1.020 ± 0.069 (stat. $\oplus$ sys.) $^{+0.045}_{-0.047}$ (br.)
	γ_s
H1	0.36 ± 0.10 (stat.) ± 0.01 (syst.) ± 0.08 (br. $\oplus$ theo.)
ZEUS	0.225 ± 0.03 (stat.) $^{+0.018}_{-0.007}$ (syst.) $^{+0.034}_{-0.026}$ (br.)
e^+e^- av.	0.259 ± 0.023 (stat. $\oplus$ syst.) $^{+0.087}_{-0.052}$ (br.)
	P_v^d
H1	0.693 ± 0.045 (stat.)± 0.004 (syst.) ± 0.009 (br.$\oplus$ theo.)
ZEUS	0.617 ± 0.038 (stat.) $^{+0.017}_{-0.009}$ (syst.)± 0.017 (br.)
e^+e^- av.	0.614 ± 0.019 (stat.$\oplus$syst.)$^{+0.023}_{-0.025}$ (br.)

17.8.2. ***Bottom quark fragmentation*** : Experimental studies of the fragmentation function for b quarks, shown in Fig. 17.9(b), have been performed at LEP and SLD [122,131,144]. Commonly used methods identify the B meson through its semileptonic decay or based upon tracks emerging from the B secondary vertex. The most recent studies [131] fit the B spectrum using a Monte Carlo shower model supplemented with non-perturbative fragmentation functions yielding consistent results.

The experiments measure primarily the spectrum of B mesons. This defines a fragmentation function which includes the effect of the decay of higher mass excitations, like the B^* and B^{**}. In the literature, there is sometimes ambiguity in what is defined to be the bottom fragmentation function. Instead of using what is directly measured (*i.e.*, the B meson spectrum) corrections are applied to account for B^* or B^{**} production in some cases. For a more detailed discussion see [1].

Heavy-flavor production in e^+e^- collisions is the primary source of information for the role of fragmentation effects in heavy-flavor production in hadron-hadron and lepton-hadron collisions. The QCD calculations tend to underestimate the data in certain regions of phase space. Recently, it was also pointed out [145] that the long-standing discrepancy between theoretical calculations and the measured B meson spectrum at the hadron colliders [146] was substantially reduced if a correct use of available information

on heavy flavor production from e^+e^- data was made.

Both bottomed- and charmed-mesons spectra have been measured recently at the TEVATRON with unprecedented accuracy [147]. The measured spectra are in good agreement with QCD calculations (including non-perturbative fragmentation effects inferred from e^+e^- data [148]), no longer supporting the previously reported discrepancies [146].

The HERA collaborations have produced a number of measurements of beauty production [139,149]. Compared with LEP data, there is at present insufficient statistical precision to make detailed measurements of the fragmentation properties of b-quarks in lepton-hadron scattering. The data which do exist have been tested against QCD-based models implementing Peterson *et al.* [114] fragmentation.

17.8.3. ***Gluon splitting into heavy quarks*** : Besides degrading the fragmentation function by gluon radiation, QCD evolution can also generate soft heavy quarks, increasing in the small x region as s increases. Several theoretical studies are available on the issue of how often $b\bar{b}$ or $c\bar{c}$ pairs are produced indirectly, via a gluon splitting mechanism [150–152]. Experimental results from studies on charm production via gluon splitting and measurements of $g \to b\bar{b}$ are given in Table 17.2.

Table 17.2: Measured fraction of events containing $g \to c\overline{c}$ and $g \to b\overline{b}$ subprocesses in Z decays, compared with theoretical predictions. The central/lower/upper values for the theoretical predictions are obtained with $m_c = (1.5 \pm 0.3)$ and $m_b = (4.75 \pm 0.25)\,\mathrm{GeV}$.

	$\overline{n}_{g\to c\overline{c}}$ (%)	$\overline{n}_{g\to b\overline{b}}$ (%)
ALEPH	[133] $3.26 \pm 0.23 \pm 0.42$	[153] $0.2777 \pm 0.042 \pm 0.057$
DELPHI		[154] $0.21 \pm 0.11 \pm 0.09$
L3	[155] $2.45 \pm 0.29 \pm 0.53$	
OPAL	[156] $3.20 \pm 0.21 \pm 0.38$	
SLD		[157] $0.307 \pm 0.071 \pm 0.066$
Theory [151]		
$\Lambda^{(5)}_{\overline{\mathrm{MS}}} = 150\,\mathrm{MeV}$	$1.35^{+0.48}_{-0.30}$	0.20 ± 0.02
$\Lambda^{(5)}_{\overline{\mathrm{MS}}} = 300\,\mathrm{MeV}$	$1.85^{+0.69}_{-0.44}$	0.26 ± 0.03

In Ref. 151, an explicit calculation of these quantities has been performed. Using these results, charm and bottom multiplicities as reported in Table 17.2 for different values of the masses and of $\Lambda^{(5)}_{\overline{\mathrm{MS}}}$ were computed in Ref. 158. The averaged experimental result for charm, taking correlations into account, $(2.96 \pm 0.38)\%$ [159] is 1–2 standard deviations

above the theoretical prediction, preferring lower values of the quark mass and/or a larger value of $\Lambda^{(5)}_{\overline{\rm MS}}$. However, higher-order corrections may well be substantial at the charm quark mass scale. Better agreement is achieved for bottom.

As reported in Ref. 151, Monte Carlo models are in qualitative agreement with these results, although the spread of the values they obtain is somewhat larger than the theoretical error estimated by the direct calculation. In particular, for charm one finds that while HERWIG [85] and JETSET [72] agree quite well with the theoretical calculation, ARIADNE [160] is higher by roughly a factor of 2, and thus is in better agreement with data. For bottom, agreement between theory, models and data is adequate. For a detailed discussion see Ref. 161.

The discrepancy with the charm prediction may be due to experimental cuts forcing the final state configuration to be more 3-jet like, which increases the charm multiplicity. Calculations that take this possibility into account are given in Ref. 152.

References:

1. O. Biebel, P. Nason, and B.R. Webber, Bicocca-FT-01-20, Cavendish-HEP-01/12, MPI-PhE/2001-14, `hep-ph/0109282`.
2. W. Kittel and E.A. De Wolf, *Soft Multihadron Dynamics*, World Scientific, Singapore (2005).
3. H.F. Jones, Nuovo Cimento **40A**, 1018 (1965);
   R.P. Feynman, *Photon Hadron Interacations*, W.A. Benjamin, New York (1972);
   Yu.L. Dokshitzer *et al.*, *Perturbative Quantum Chromodynamics*, ed. A.H. Mueller, World Scientific, Singapore (1989);
   K.H. Streng, Z. Phys. **C2**, 377 (1994).
4. V.N. Gribov and L.N. Lipatov, Sov. J. Nucl. Phys. **15**, 438 (1972);
   L.N. Lipatov, Sov. J. Nucl. Phys. **20**, 95 (1975);
   G. Altarelli and G. Parisi, Nucl. Phys. **B126**, 298 (1977);
   Yu.L. Dokshitzer, Sov. Phys. JETP **46**, 641 (1977).
5. P. Nason and B.R. Webber, Nucl. Phys. **B421**, 473 (1994);
   Erratum *ibid.*, **B480**, 755 (1996).
6. W. Furmanski and R. Petronzio, preprint TH.2933–CERN (1980), Phys. Lett. **97B**, 437 (1980).
7. G. Curci *et al.*, Nucl. Phys. **B175**, 27 (1980);
   E.G. Floratos *et al.*, Nucl. Phys. **B192**, 417 (1981);
   J. Kalinowski *et al.*, Nucl. Phys. **B181**, 221 (1981);
   J. Kalinowski *et al.*, Nucl. Phys. **B181**, 253 (1981).
8. R.K. Ellis, J. Stirling, and B.R. Webber: *QCD and Collider Physics*, Cambridge University Press, Cambridge (1996).
9. ALEPH Collab.: D. Buskulic *et al.*, Z. Phys. **C73**, 409 (1997).
10. ALEPH Collab.: E. Barate *et al.*, Phys. Rev. **294**, 1 (1998).
11. AMY Collab.: Y.K. Li *et al.*, Phys. Rev. **D41**, 2675 (1990).
12. DELPHI Collab.: P. Abreu *et al.*, Eur. Phys. J. **C6**, 19 (1999).
13. HRS Collab.: D.Bender *et al.*, Phys. Rev. **D31**, 1 (1984).
14. L3 Collab.: B. Adeva *et al.*, Phys. Lett. **B259**, 199 (1991).

15. MARK II Collab.: G.S. Abrams *et al.*, Phys. Rev. Lett. **64**, 1334 (1990).
16. MARK II Collab.: A. Petersen *et al.*, Phys. Rev. **D37**, 1 (1988).
17. OPAL Collab.: R. Akers *et al.*, Z. Phys. **C72**, 191 (1996).
18. OPAL Collab.: K. Ackerstaff *et al.*, Z. Phys. **C75**, 193 (1997).
19. OPAL Collab.: K. Ackerstaff *et al.*, Eur. Phys. J. **C7**, 369 (1998).
20. OPAL Collab.: G. Abbiendi *et al.*, Eur. Phys. J. **C16**, 185 (2000); OPAL Collab.: G. Abbiendi *et al.*, Eur. Phys. J. **C27**, 467 (2003).
21. OPAL Collab.: G. Abbiendi *et al.*, Eur. Phys. J. **C37**, 25 (2004).
22. SLD Collab.: K. Abe *et al.*, Phys. Rev. **D69**, 072003 (2004).
23. TASSO Collab.: R. Brandelik *et al.*, Phys. Lett. **B114**, 65 (1982).
24. TASSO Collab.: W. Braunschweig *et al.*, Z. Phys. **C47**, 187 (1990).
25. TPC Collab.: H. Aihara *et al.*, Phys. Rev. Lett. **61**, 1263 (1988).
26. ALEPH Collab.: D. Barate *et al.*, Phys. Lett. **B357**, 487 (1995); Erratum *ibid.*, **B364**, 247 (1995).
27. DELPHI Collab.: P. Abreu *et al.*, Phys. Lett. **B311**, 408 (1993).
28. DELPHI Collab.: P. Abreu *et al.*, Phys. Lett. **B398**, 194 (1997).
29. DELPHI Collab.: P. Abreu *et al.*, Eur. Phys. J. **C13**, 573 (2000); W. de Boer and T. Kußmaul, IEKP-KA/93-8, `hep-ph/`9309280.
30. B.A. Kniehl, G. Kramer, and B. Pötter, Phys. Rev. Lett. **85**, 5288 (2001).
31. E665 Collab.: M.R. Adams *et al.*, Phys. Lett. **B272**, 163 (1991).
32. EMC Collab.: M. Arneodo *et al.*, Z. Phys. **C35**, 417 (1987).
33. H1 Collab.: I. Abt *et al.*, Z. Phys. **C63**, 377 (1994).
34. ZEUS Collab.: M. Derrick *et al.*, Z. Phys. **C70**, 1 (1996).
35. ZEUS Collab.: J. Breitweg *et al.*, Phys. Lett. **B414**, 428 (1997).
36. H1 Collab.: S. Aid *et al.*, Nucl. Phys. **B445**, 3 (1995).
37. ZEUS Collab.: M. Derrick *et al.*, Z. Phys. **C67**, 93 (1995).
38. H1 Collab.: C. Adloff *et al.*, Nucl. Phys. **B504**, 3 (1997).
39. ZEUS Collab.: J. Breitweg *et al.*, Eur. Phys. J. **C11**, 251 (1999).
40. H1 Collab.: F.D. Aaron *et al.*, Phys. Lett. **B654**, 148 (2007).
41. MARK II Collab.: J.F. Patrick *et al.*, Phys. Rev. Lett. **49**, 1232, (1982).
42. D. Graudenz, CERN-TH/96-52.
43. P. Dixon *et al.*, J. Phys. **G25**, 1453 (1999).
44. Yu.L. Dokshitzer *et al.*, *Basics of Perturbative QCD*, Editions Frontières, Paris (1991).
45. C.P. Fong and B.R. Webber, Nucl. Phys. **B355**, 54 (1992).
46. DELPHI Collab.: P. Abreu *et al.*, Z. Phys. **C73**, 11 (1996).
47. DELPHI Collab.: P. Abreu *et al.*, Z. Phys. **C73**, 229 (1997).
48. L3 Collab.: P. Achard *et al.*, Phys. Reports **399**, 71 (2004).
49. TOPAZ Collab.: R. Itoh *et al.*, Phys. Lett. **B345**, 335 (1995).
50. OPAL Collab.: M.Z. Akrawy *et al.*, Phys. Lett. **B247**, 617 (1990).
51. TASSO Collab.: W. Braunschweig *et al.*, Z. Phys. **C22**, 307 (1990).
52. BES Collab.: J.Z. Bai *et al.*, Phys. Rev. **D69**, 072002 (2004).
53. ALEPH Collab.: D. Buskulic *et al.*, Z. Phys. **C55**, 209 (1992).
54. ALEPH Collab.: A. Heister *et al.*, Eur. Phys. J. **C35**, 457 (2004).

55. DELPHI Collab.: P. Abreu *et al.*, Phys. Lett. **B275**, 231 (1992).
56. DELPHI Collab.: P. Abreu *et al.*, Eur. Phys. J. **C5**, 585 (1998).
57. DELPHI Collab.: P. Abreu *et al.*, Phys. Lett. **B459**, 397 (1999).
58. L3 Collab.: M. Acciarri *et al.*, Phys. Lett. **B444**, 569 (1998).
59. TPC/TWO-GAMMA Collab.: H. Aihara *et al.*, "*Charged Hadron Production in e^+e^- Annihilation at $\sqrt{s} = 29$ GeV*," LBL 23737.
60. OPAL Collab.: R. Akers *et al.*, Z. Phys. **C86**, 203 (1995).
61. J. Binnewies, Hamburg University PhD Thesis, DESY 97-128, `hep-ph/9707269`.
62. ALEPH Collab.: R. Barate *et al.*, Eur. Phys. J. **C17**, 1 (2000);
    OPAL Collab.: R. Akers *et al.*, Z. Phys. **C68**, 179 (1995);
    OPAL Collab.: G. Abbiendi *et al.*, Eur. Phys. J. **C11**, 217 (1999).
63. COMPASS Collab.: G. Baum *et al.*, CERN-SPSLC-96-14;
    CERN-SPSLC-P-297.
64. HERMES Collab.: A. Airapetian *et al.*, Phys. Rev. **D71**, 012003 (2005).
65. SMC Collab.: B. Adeva *et al.*, Phys. Lett. **B420**, 180, (1998).
66. J. Binnewies *et al.*, Phys. Rev. **D52**, 4947 (1995);
    Z. Phys. **C65**, 471 (1995).
67. B.A. Kniehl *et al.*, Nucl. Phys. **B582**, 514 (2000).
68. S.Albino *et al.*, Nucl. Phys. **B725**, 181, (2005);
    ibid., **B734**, 50 (2006).
69. S. Kretzer, Phys. Rev. **D62**, 054001 (2000).
70. L. Bourhis *et al.*, Eur. Phys. J. **C19**, 89 (2001).
71. S. Kretzer *et al.*, Eur. Phys. J. **C22**, 269 (2001).
72. T. Sjöstrand and M. Bengtsson, Comp. Phys. Comm. **43**, 367 (1987);
    T. Sjöstrand, Comput. Phys. Commun. **82**, 74 (1994).
73. P.J. Mulders and R.D. Tangerman, Nucl. Phys. **B461**, 197 (1996);
    Erratum *ibid.*, **B484**, 538 (1997).
74. R. Jacob, Nucl. Phys. **A711**, 35 (2002).
75. J.P. Ralston and D.E. Soper, Nucl. Phys. **B152**, 109 (1979).
76. J. Collins, Nucl. Phys. **B396**, 161 (1993).
77. CLAS Collab.: H. Avakian *et al.*, Phys. Rev. **D69**, 112004 (2004);
    HERMES Collab.: A. Airapetian *et al.*, Phys. Rev. Lett. **84**, 4047 (2000);
    HERMES Collab.: A. Airapetian *et al.*, Phys. Rev. **D64**, 097101 (2001).
78. D. Sivers, Phys. Rev. **D43**, 261 (1991).
79. HERMES Collab.: A. Airapetian *et al.*, Phys. Rev. Lett. **94**, 012002 (2005).
80. COMPASS Collab.: V.Y Alexakhin *et al.*, Phys. Rev. Lett. **94**, 202002 (2005).
81. COMPASS Collab.: V.Y Alexakhin *et al.*, Nucl. Phys. **B765**, 31 (2007).
82. X. Artru and G. Mennessier, Nucl. Phys. **B70**, 93 (1974).
83. B. Andersson *et al.*, Phys. Reports **97**, 31 (1983).
84. S. Chun and C. Buchanan, Phys. Reports **292**, 239 (1998).
85. G. Marchesini *et al.*, Comput. Phys. Commun. **67**, 465 (1992);
    G. Corcella *et al.*, JHEP **0101**, 010 (2001).
86. OPAL Collab.: G. Alexander *et al.*, Z. Phys. **C69**, 543 (1996).
87. M. Schmelling, Phys. Script. **51**, 683 (1995).

88. D. Amati and G. Veneziano, Phys. Lett. **B83**, 87 (1979).
89. ALEPH Collab.: D. Buskulic *et al.*, Z. Phys. **C66**, 355 (1995);
ARGUS Collab.: H. Albrecht *et al.*, Z. Phys. **C44**, 547 (1989);
OPAL Collab.: R. Akers *et al.*, Z. Phys. **C63**, 181 (1994);
SLD Collab.: K. Abe *et al.*, Phys. Rev. **D59**, 052001 (1999).
90. B.A. Kniehl *et al.*, Nucl. Phys. **B597**, 337 (2001).
91. E665 Collab.: M.R. Adams *et al.*, Z. Phys. **C61**, 539 (1994).
92. EMC Collab.: J.J. Aubert *et al.*, Z. Phys. **C18**, 189 (1983);
EMC Collab.: M. Arneodo *et al.*, Phys. Lett. **B150**, 458 (1985).
93. EMC Collab.: M. Arneodo *et al.*, Z. Phys. **C33**, 167 (1986).
94. EMC Collab.: M. Arneodo *et al.*, Z. Phys. **C34**, 283 (1987).
95. HERMES Collab.: A. Airapetian *et al.*, Eur. Phys. J. **C21**, 599 (2001).
96. T.P. M$^{\rm c}$Pharlin *et al.*, Phys. Lett. **B90**, 479 (1980).
97. H1 Collab.: S. Aid *et al.*, Nucl. Phys. **B480**, 3 (1996).
98. H1 Collab.: C. Adloff *et al.*, Eur. Phys. J. **C18**, 293 (2000);
H1 Collab.: A. Aktas *et al.*, Eur. Phys. J. **C36**, 413 (2004).
99. ZEUS Collab.: M. Derrick *et al.*, Z. Phys. **C68**, 29 (1995);
ZEUS Collab.: J. Breitweg *et al.*, Eur. Phys. J. **C2**, 77 (1998).
100. ZEUS Collab.: S. Chekanov *et al.*, Phys. Lett. **B553**, 141 (2003).
101. ZEUS Collab.: S. Chekanov *et al.*, Nucl. Phys. **B786**, 121 (2007).
102. S. Albino *et al.*, Phys. Rev. **D75**, 034018, (2007).
103. OPAL Collab.: P.D. Acton *et al.*, Phys. Lett. **B305**, 407 (1993).
104. E632 Collab.: D. DeProspo *et al.*, Phys. Rev. **D50**, 6691 (1994).
105. ZEUS Collab.: S. Chekanov *et al.*, Eur. Phys. J. **C51**, 1 (2007).
106. G. Grindhammer *et al.*, in: *Proceedings of the Workshop on Monte Carlo Generators for HERA Physics*, Hamburg, Germany, 1998/1999.
107. N. Brook *et al.*, in: *Proceedings of the Workshop for Future HERA Physics at HERA*, Hamburg, Germany, 1996.
108. V.A. Khoze *et al.*, *Proceedings, Conference on High-Energy Physics, Tbilisi 1976*;
J.D. Bjorken, Phys. Rev. **D17**, 171 (1978).
109. B. Mele and P. Nason, Phys. Lett. **B245**, 635 (1990);
Nucl. Phys. **B361**, 626 (1991).
110. Yu.L. Dokshitzer *et al.*, Phys. Rev. **D53**, 89 (1996).
111. M. Cacciari and S. Catani, Nucl. Phys. **B617**, 253 (2001).
112. P. Nason and C. Oleari, Phys. Lett. **B418**, 199 (1998);
ibid., **B447**, 327 (1999);
Nucl. Phys. **B565**, 245 (2000).
113. K. Melnikov and A. Mitov, Phys. Rev. **D70**, 034027 (2004).
114. C. Peterson *et al.*, Phys. Rev. **D27**, 105 (1983).
115. V.G. Kartvelishvili *et al.*, Phys. Lett. **B78**, 615 (1978).
116. P. Collins and T. Spiller, J. Phys. **G11**, 1289 (1985).
117. G. Colangelo and P. Nason, Phys. Lett. **B285**, 167 (1992).
118. M.G. Bowler, Z. Phys. **C11**, 169 (1981).
119. E. Braaten *et al.*, Phys. Rev. **D51**, 4819 (1995).

120. OPAL Collab.: R. Akers *et al.*, Z. Phys. **C67**, 27 (1995).
121. ARGUS Collab.: H. Albrecht *et al.*, Z. Phys. **C52**, 353 (1991).
122. ALEPH Collab.: D. Buskulic *et al.*, Phys. Lett. **B357**, 699 (1995).
123. J. Chrin, Z. Phys. **C36**, 163 (1987).
124. R.L. Jaffe and L. Randall, Nucl. Phys. **B412**, 79 (1994);
P. Nason and B. Webber, Phys. Lett. **B395**, 355 (1997).
125. M. Cacciari and E. Gardi, Nucl. Phys. **B664**, 299 (2003).
126. L. Randall and N. Rius, Nucl. Phys. **B441**, 167 (1995).
127. CLEO Collab.: M. Artuso *et al.*, Phys. Rev. **D70**, 112001 (2004).
128. BELLE Collab.: R. Seuster *et al.*, Phys. Rev. **D73**, 032002 (2006).
129. CLEO Collab.: R.A. Briere *et al.*, Phys. Rev. **D62**, 112003 (2000).
130. BABAR Collab.: B. Aubert *et al.*, Phys. Rev. **D65**, 0911004 (2002).
131. ALEPH Collab.: A. Heister *et al.*, Phys. Lett. **B512**, 30 (2001);
OPAL Collab.: G. Abbiendi *et al.*, Eur. Phys. J. **C29**, 463 (2003);
SLD Collab.: K. Abe *et al.*, Phys. Rev. **D65**, 092006 (2002);
Erratum *ibid.*, **D66**, 079905 (2002).
132. CLEO Collab.: D. Bortoletto *et al.*, Phys. Rev. **D37**, 1719 (1988).
133. ALEPH Collab.: R. Barate *et al.*, Phys. Lett. **B561**, 213 (2003).
134. ARGUS Collab.: H. Albrecht *et al.*, Z. Phys. **C54**, 1 (1992).
135. LEP Collab. and the LEP and SLD electroweak and heavy flavour working groups, `hep-ex/0412015`.
136. M. Cacciari *et al.*, JHEP **0604**, 006 (2006).
137. M. Dasgupta and B.R. Webber, Nucl. Phys. **B484**, 247 (1997).
138. H1 Collab.: C. Adloff *et al.*, Nucl. Phys. **B520**, 191 (2001);
H1 Collab.: C. Adloff *et al.*, Phys. Lett. **B528**, 199 (2002);
H1 Collab.: A. Aktas *et al.*, Eur. Phys. J. **C40**, 56 (2005);
H1 Collab.: A. Aktas *et al.*, Eur. Phys. J. **C45**, 23 (2006);
ZEUS Collab.: J. Breitweg *et al.*, Phys. Lett. **B481**, 213 (2000);
ZEUS Collab.: S. Chekanov *et al.*, Phys. Lett. **B545**, 244 (2002);
ZEUS Collab.: S. Chekanov *et al.*, Nucl. Phys. **B672**, 3 (2003);
ZEUS Collab.: S. Chekanov *et al.*, Phys. Lett. **B590**, 143 (2004);
ZEUS Collab.: S. Chekanov *et al.*, Phys. Rev. **D69**, 012004 (2004).
139. H1 Collab.: A. Aktas *et al.*, Phys. Lett. **B621**, 56 (2005).
140. H1 Collab.: A. Aktas *et al.*, Eur. Phys. J. **C38**, 447 (2005).
141. ZEUS Collab.: S. Chekanov *et al.*, Eur. Phys. J. **C44**, 351 (2005).
142. ZEUS Collab.: S. Chekanov *et al.*, JHEP **0707**, 074 (2007).
143. L. Gladillin, `hep-ex/9912064`.
144. L3 Collab.: B. Adeva *et al.*, Phys. Lett. **B261**, 177 (1991).
145. M. Cacciari and P. Nason, Phys. Rev. Lett. **89**, 122003 (2002).
146. CDF Collab.: F. Abe *et al.*, Phys. Rev. Lett. **71**, 500 (1993);
CDF Collab.: F. Abe *et al.*, Phys. Rev. Lett. **71**, 2396 (1993);
CDF Collab.: F. Abe *et al.*, Phys. Rev. **D50**, 4252 (1994);
CDF Collab.: F. Abe *et al.*, Phys. Rev. Lett. **75**, 1451 (1995);
CDF Collab.: D. Acosta *et al.*, Phys. Rev. **D66**, 032002 (2002);

CDF Collab.: D. Acosta *et al.*, Phys. Rev. **D65**, 052005 (2002);
D0 Collab.: S. Abachi *et al.*, Phys. Rev. Lett. **74**, 3548 (1995);
UA1 Collab.: C. Albajar *et al.*, Phys. Lett. **B186**, 237 (1987);
UA1 Collab.: C. Albajar *et al.*, Phys. Lett. **B256**, 121 (1991);
Erratum *ibid.*, **B272**, 497 (1991).
147. CDF Collab.: D. Acosta *et al.*, Phys. Rev. Lett. **91**, 241804 (2003);
CDF Collab.: D. Acosta *et al.*, Phys. Rev. **D71**, 032001 (2005).
148. M. Cacciari and P. Nason, JHEP **0309**, 006 (2003);
M. Cacciari *et al.*, JHEP **0407**, 033 (2004);
B.A. Kniehl *et al.*, Phys. Rev. Lett. **96**, 012001 (2006).
149. H1 Collab.: C. Adloff *et al.*, Phys. Lett. **B467**, 156 (1999);
H1 Collab.: A. Aktas *et al.*, Eur. Phys. J. **C41**, 453 (2005);
ZEUS Collab.: J. Breitweg *et al.*, Eur. Phys. J. **C18**, 625 (2001);
ZEUS Collab.: S. Chekanov *et al.*, Phys. Lett. **B599**, 173 (2004).
150. A.H. Mueller and P. Nason, Nucl. Phys. **B266**, 265 (1986);
M.L. Mangano and P. Nason, Phys. Lett. **B285**, 160 (1992).
151. M.H. Seymour, Nucl. Phys. **B436**, 163 (1995).
152. D.J. Miller and M.H. Seymour, Phys. Lett. **B435**, 213 (1998).
153. ALEPH Collab.: R. Barate *et al.*, Phys. Lett. **B434**, 437 (1998).
154. DELPHI Collab.: P. Abreu *et al.*, Phys. Lett. **B405**, 202 (1997).
155. L3 Collab.: M. Acciarri *et al.*, Phys. Lett. **B476**, 243 (2000).
156. OPAL Collab.: G. Abbiendi *et al.*, Eur. Phys. J. **C13**, 1 (2000).
157. SLD Collab.: K. Abe *et al.*, SLAC-PUB-8157, `hep-ex/9908028`.
158. S. Frixione *et al.*, Heavy Quark Production, in A.J. Buras and M. Lindner (eds.), *Heavy flavours II*, World Scientific, Singapore (1998), `hep-ph/9702287`.
159. A. Giammanco, in: *Proceedings of the XII International Workshop on Deep Inelastic Scattering* DIS'2004, Štrbské Pleso, Slovakia.
160. L. Lönnblad, Comp. Phys. Comm. **71**, 15 (1992).
161. A. Ballestrero *et al.*, CERN-2000-09-B, `hep-ph/0006259`.